Random Phase Center Motion Technique for Enhanced Angle-Doppler Discrimination Using MIMO Radars

Christian Hammes* †, Bhavani Shankar M. R.*, Yogesh Nijsure*, Thiemo Spielmann‡ and Björn Ottersten*

*University of Luxembourg, SnT, ‡ IEE Contern †Email: christian.hammes@uni.lu

Abstract—A random Phase Center Motion (PCM) technique is presented in this paper, based on Frequency Modulated Continuous Wave (FMCW) radar, in order to suppress the angle-Doppler coupling in Time Division Multiplex (TDM) Multiple-Input-Multiple-Output (MIMO) radar when employing sparse array structures. The presented approach exploits an *apparently* moving transmit platform or PCM due to spatio-temporal transmit array modulation. In particular, the work considers a framework utilizing a random PCM trajectory. The statistical characterization of the random PCM trajectory is devised, such that the PCM and the target motion coupling is minimal, while the angular resolution is increased by enabling the virtual MIMO concept. In more details, this paper discusses sidelobe suppression approaches within the angle-Doppler Ambiguity Function (AF) by introducing a phase center probability density function within the array. This allows for enhanced discrimination of multiple targets. Simulation results demonstrate the suppression angle-Doppler coupling by more than 30 dB, even though spatio-temporal transmit array modulation is done across chirps which leads usually to strong angle-Doppler coupling.

I. INTRODUCTION

Sparse array structures have attracted a lot of attention within Multiple-Input-Multiple-Output (MIMO) radar research, since they are cheaper than their dense array counterparts of the same apertures due to lower system components. The key motivation for using sparse array structures is its capability for transmitting orthogonal sequences from each transmitting element, such that the receiver can discriminate between the different radiation origins and a filled array can be virtually constructed [1]. A low cost approach of achieving orthogonality among different transmitters is the utilization of Time Division Multiplex (TDM) MIMO, where only one transmitter is active at a time and therefore the transmitted signals are orthogonal with respect to time. Works like [2] have developed a low cost Frequency Modulated Continuous Wave (FMCW) radar by switching the transmitters and receivers across FMCW chirps in a linear fashion. The consecutive switching scheme of transmit-receive-pairs yields a simple Discrete Fourier Transform (DFT) based received processing for resolving different angle of arrivals. The sidelobe suppression of the backscatter is addressed by virtual antenna overlapping; this decreases the virtual array aperture and therefore the angular resolution [2]. The authors in [3] have used a linear switching scheme like [2] in an inter-chirp modulated mechanism. This is mainly because linear switching of antenna elements across pulses results into angle-Doppler

coupling [2].

Works like [4]-[7] have addressed the aforementioned coupling problem. In [4], range-Doppler map is derived from the usage of a single transmitting antenna, such that the target Doppler can be extracted and the TDM modulated signal is compensated by the Doppler shift of the moving target. The authors in [5] and [6] introduce an intra-chirp modulation scheme, where the antenna elements are switched quite fast and the phase variations due to TDM is much faster than the phase variations due to the target motion. Therefore the angular information decouples from the Doppler information. However, the intra-chirp TDM requires increased hardware complexity, like faster switches and a second FMCW modulator [5].

All the aforementioned approaches have been used in linear TDM, while a nonlinear approach has been introduced in [7]. The authors in [7] have utilized the TDM technique as a virtual motion of the transmit phase center, called Phase Center Motion (PCM). The PCM techniques has been introduced as a joint transmit-receive-time modulated array approach, where the PCM is independent of the target motion and, therefore, enables unambiguous multiple target discrimination by using inter-chirp modulation.

Other approaches of time modulated arrays have been investigated in works like [8]-[12], where the apparent motion of the phase center is analyzed within an angle-Doppler plane. While time modulated or four dimensional arrays are exploiting apparent antenna motion in an attempt to optimize the radiation pattern sidelobes, the PCM approach in [7] exploits the time modulation such that a sparse array structure provides thumbtack response within the angle-Doppler domain, called angle-Doppler Ambiguity Function (AF). The authors in [8] and [9] have presented bidirectional and unidirectional PCM, respectively, in order to suppress the array radiation pattern sidelobes. A differential evolution algorithm is introduced in [10], for radiation pattern optimization. Works like [11] have applied pulse shifting techniques for synthesizing the radiation pattern. A study on FMCW chirps in time modulated arrays has been elaborated in [12].

This work builds on the PCM approach of [7] and the key contributions are described below. In contrast to the deterministic PCM in[7], the current work develops a framework for PCM trajectories where the phase center position varies *randomly* in time. The paper utilizes random PCM trajectories whose statistical characterization is based on uncorrelated transitions.
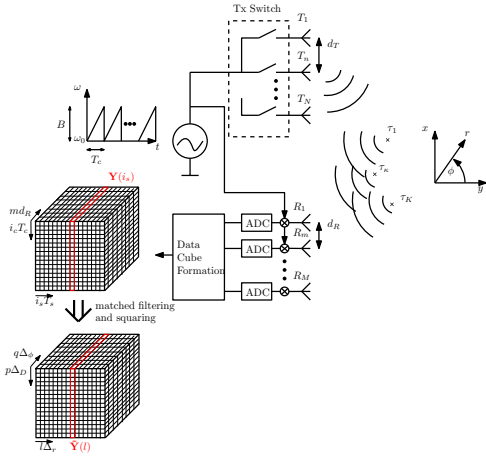
Fig. 1. FMCW System Diagram for white PCM modulation. The matrix $\tilde{\mathbf{Y}}$ denotes the angle-Doppler ambiguity function for a particular range bin.

Such a PCM implies high trajectory fluctuations, which are different from smooth target trajectories, due to the inertia of real targets. Therefore, PCM and the target trajectory can be decoupled due to their independent trajectories. In addition to the uncorrelated transitions, the PCM is described by the Probability Density Function (PDF). An interesting aspect is that the PDF impacts the angle-Doppler determination. A second contribution of this work lies in the exploitation of the PDF to enhance target discrimination. Since the PCM trajectory parameters are known, a trajectory matched filter bank can be employed in order to extract Doppler and angular information. A third contribution of the paper is the development of a matched filter operating on the FMCW samples, chirps and the number of antennas to provide multiple target information. Throughout the work, the operator $\|\cdot\|$ is used for the l_2-norm. $[\cdot]_{\eta,\gamma}$ defines a matrix entry with row index η and column index γ. The notation $[\cdot]_\eta$ indicates a column vector element with the index η. The $E\{\cdot\}$ is the expectation operator. The symbol $\mathbb{C}$ defines the set of complex numbers.

II. SYSTEM MODEL

The underlying system is based on FMCW scheme as depicted in Figure 1. The local oscillator output is a consecutive set of FMCW chirps, where each chirp is radiated in a random alternating fashion with just one transmit antenna element being active at a time. The collocated transmit antenna elements are mounted along the x-axis with an inter-element spacing of d_T and a total number of N antenna elements. From the sparse transmit array structure the chirp sequence is propagating towards K multiple, in general moving, point scatters. The back-scattered signal, which is a superposition of single target back-scatters, is captured by the dense receive array. The receive array contains M collocated antenna elements with an inter-element spacing of d_R. Due to the FMCW scheme, the captured signal at each receiver is down-mixed by an instantaneous local oscillator signal and subsequently converted to the digital domain. The accumulated data is rearranged in a data-cube, where the first dimension contains

the intra-chirp samples, the second dimension denotes the inter-chirp samples and the third dimension refers to the data from each receive antenna element. A matched filter is applied to each dimension in order to compress the continuous wave such that the range, angle and Doppler information can be extracted. The matched filter output squaring provides the range-angle-Doppler AF.

A. Transmitted Signal

The transmitted signal $\mathbf{u} \in \mathbb{C}^{\mathcal{I}_c \times 1}$ consists of $\mathcal{I}_c$ FMCW chirps, while each chirp contains a different phase center position $\chi(i_c)$ at the transmit array. The switching across chirps is denoted by the chirp index i_c,

$$[\mathbf{u}]_{i_c}(t) = \exp\left(jk_\phi\chi(i_c)\right)\exp\left(j\left(\omega_0 t + \frac{B}{2T_c}t^2\right)\right). \quad (1)$$

Since the antenna elements are assumed to be point-like isotropic radiators mounted in x-direction, the propagation vector for x-direction is denoted as $k_\phi = k_0\sin(\phi)$, where k_0 is the free space wave number and j the complex number. The FMCW parameters are the center angular frequency ω_0, the angular bandwidth B and the chirp duration T_c.

B. Received Signal

The received signal is sampled by the intra-chirps sampling time is denoted by T_s, while i_s describes the intra-chirp sample index. If the signal is reflected by multiple point-like moving targets, the captured down-mixed and digital converted received signals are written in matrix notation $\mathbf{Y} \in \mathbb{C}^{\mathcal{I}_c \times M}$,

$$[\mathbf{Y}]_{i_c,m}(i_s) = \sum_{\kappa=1}^{K} c_\kappa \exp\left(jk_{\phi_\kappa}d_R m\right)\exp\left(jk_{\phi_\kappa}\chi(i_c)\right) \quad (2)$$
$$\times \exp\left(j\left(\omega_{D_\kappa}(i_c T_c + i_s T_s) + \omega_{B_\kappa}i_s T_s\right)\right).$$

The complex constant $c_\kappa = \sigma_\kappa \exp\left(j\left(\omega_0 + \omega_{D_\kappa}\right)t_\kappa + j\frac{B}{2T_c}t_\kappa^2\right)$, which is a result of the FMCW down-mixing procedure and propagation effects, contains the κ-th target radar cross section together with the signal attenuation σ_κ. The propagation delay $t_\kappa = \frac{2r_\kappa}{c_0}$ includes the target range r_κ and speed of light c_0. The κ-th target moves continuously during the coherent processing interval, therefore the Doppler shift ω_{D_κ} appears in the entire sequence considered by the term $\omega_{D_\kappa}(i_c T_c + i_s T_s)$. The sampling time and the corresponding sample index are denoted by T_s and i_s, respectively. The FMCW associated angular beat frequency is defined as $\omega_{B_\kappa} = 2\frac{B}{T_c}\frac{r_\kappa}{c_0}$.

C. Trajectory Matched Filter

After the formation of data-cube, a three dimensional matched filter is applied with a subsequent squaring. Using the model (2), the matched filter operation in i_s and m directions has the form of a Discrete Fourier Transform (DFT). The matched filter for the inter-chirp dimension i_c is more involved since it has to extract Doppler and angular information simultaneously. Further, during this extraction, the angular information in i_c direction has to be

synchronized with the angular information in m direction. The synchronization problem is solved by zero padding in m dimension such that the spatial DFT wave number resolution is proportional to the inverse virtual array size. The angular resolution depends on the virtual array size $\Delta_\phi = \frac{4\pi}{MN\lambda}$ [1]. The Doppler resolution is proportional to the inverse coherent processing interval $\Delta_D = \frac{2\pi}{\mathcal{I}_c T_c}$ [13] and the range resolution is defined as $\Delta_r = \frac{2\pi}{T_c}$. By reformulating the range resolution expression, the actual limiting factor for resolution is the angular bandwidth B. The squared output of the matched filter $\left[\tilde{\mathbf{Y}}\right]_{p,q}(l)$ for the p-th Doppler bin, q-th angular bin and l-th range bin is $\left[\tilde{\mathbf{Y}}\right]_{p,q}(l) =$

$\left\|\sum_{m,i_s,i_c}[\mathbf{Y}]_{i_c,m}(i_s)\exp\left\{-j\left(l\Delta_r i_s T_s + p\Delta_D i_c T_c\right)\right\}\right.$
$\left.\times \exp\left\{-j\left(q\Delta_\phi d_R m + q\Delta_\phi\chi(i_c)\right)\right\}\right\|^2$. Using (2), results in,

$$\left[\tilde{\mathbf{Y}}\right]_{p,q}(l) = \left\|\sum_{\kappa=1}^{K} c_\kappa \sum_{m=1}^{M}\exp\left(-j(q\Delta_\phi - k_{\phi_\kappa})d_R m\right)\right.$$
$$\times \sum_{i_s=1}^{\mathcal{I}_s}\exp\left(-j\left(l\Delta_r - (\omega_{B_\kappa} + \omega_{D_\kappa})\right)i_s T_s\right) \qquad (3)$$
$$\left.\times \sum_{i_c=1}^{\mathcal{I}_c}\exp\left(-j(q\Delta_\phi - k_{\phi_\kappa})\chi(i_c) - j(p\Delta_D - \omega_{D_\kappa})i_c T_c\right)\right\|^2.$$

Equation (3) illustrates the range migration due to range-Doppler coupling in the FMCW radar. Further, it can be shown, if two targets κ_1 and κ_2 are in different resolution bins, the cross terms, which are outputs of the squaring, can be neglected. Therefore the squared matched filter output can be formulated as a superposition of targets,

$$\left[\tilde{\mathbf{Y}}\right]_{p,q}(l) = \sum_{\kappa=1}^{K}\sigma_\kappa^2\left\|f_{r_\kappa}(l)\right\|^2\left\|f_{\phi_\kappa}(q)\right\|^2 \qquad (4)$$
$$\times \left\|\sum_{i_c=1}^{\mathcal{I}_c}\exp\left(-jk'_{\phi_\kappa}(q)\chi(i_c) - j\omega'_{D_\kappa}(p)i_c T_c\right)\right\|^2.$$

Conveniently, the range and angular filter response are redefined as $f_{r_\kappa}(l) = \sum_{i_s=1}^{\mathcal{I}_s}\exp\left(-j\left(l\Delta_r - (\omega_{B_\kappa} + \omega_{D_\kappa})\right)i_s T_s\right)$ and $f_{\phi_\kappa}(q) = \sum_{m=1}^{MN}\exp\left(-j(q\Delta_\phi - k_{\phi_\kappa})d_R m\right)$. Due to the squaring operation the phase term from FMCW processing vanishes and only the κ-th target attenuation factor σ_κ remains. Moreover, for the sake of convenience, the angular and Doppler coordinates are transferred to $k'_{\phi_\kappa}(q) = q\Delta_\phi - k_{\phi_\kappa}$ and $\omega'_{D_\kappa}(p) = p\Delta_D - \omega_{D_\kappa}$ respectively.
Equation (4) can be further simplified by assuming $\chi(i_c)$ to be a random process. A detailed derivation for a white random process with arbitrary PDF is demonstrated in Section III.

III. RANDOM PHASE CENTER MOTION

Unlike a deterministic function for PCM as considered in [7], the PCM $\chi(i_c)$ is considered as a random process. In particular, let $\rho_{\chi(i_c)}$ denote the PDF of $\chi(i_c)$. One phase center position is further assumed to be independent of the other, leading to Dirac-like autocorrelation response
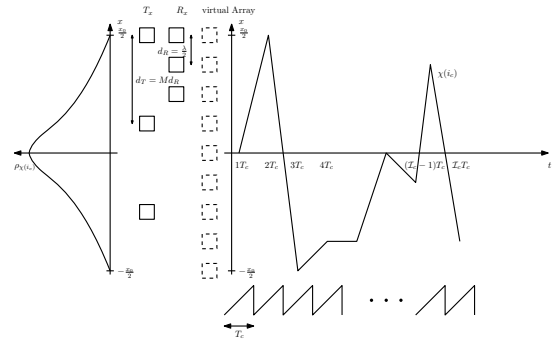
Fig. 2. Random PCM properties with the PCM PDF on left side and the uncorrelated phase center positions at the right side.

$E\left\{\chi(i_{c1})\chi(i_{c2})\right\} = \delta(i_{c1} - i_{c2})$. The generic PDF, $\rho_{\chi(i_c)}$, is assumed to be time independent. These assumptions lead to a wide sense stationary characterization of $\chi(i_c)$.

Figure 2 illustrates a snapshot of random PCM. As discussed in [7], the phase center can assume any real position within the virtual array by appropriate modulation scheme. Thus, in general, the PDF $\rho_{\chi(i_c)}$ is continuous; however, the PDF is discrete for scenarios involving antenna switching.

Since the PCM is a white random process, (4) considers an estimate of the expected matched filter output or angle-Doppler AF. Based on this, for further analysis, the average value of (4) is considered,

$$\left[\tilde{\mathbf{Y}}\right]_{p,q}(l) = \sum_{\kappa=1}^{K}\sigma_\kappa^2\left\|f_{r_\kappa}(l)\right\|^2\left\|f_{\phi_\kappa}(q)\right\|^2 \qquad (5)$$
$$\times E\left\{\left\|\sum_{i_c=1}^{\mathcal{I}_c}\exp\left(-jk'_{\phi_\kappa}(q)\chi(i_c) - j\omega'_{D_\kappa}(p)i_c T_c\right)\right\|^2\right\}.$$

The consideration of the latter term in (5) leads to an expression of a rectangular windowed periodogram,

$$f_\chi(q,p) = E\left\|\sum_{i_c=1}^{\mathcal{I}_c}\exp\left(-jk'_{\phi_\kappa}(q)\chi(i_c) - j\omega'_{D_\kappa}(p)i_c T_c\right)\right\|^2$$
$$\qquad (6)$$
$$= \sum_{i_{c1}=1}^{\mathcal{I}_c}\sum_{i_{c2}=1}^{\mathcal{I}_c}E\left\{\exp\left(-jk'_{\phi_\kappa}(q)(\chi(i_{c1}) - \chi(i_{c2}))\right)\right\}$$
$$\times \exp\left(-j\omega'_{D_\kappa}(p)(i_{c1} - i_{c2})T_c\right)$$
$$= \sum_{i=-\mathcal{I}_c}^{\mathcal{I}_c}\left(1 - \frac{|i|}{\mathcal{I}_c}\right)r(i)\exp\left(-j\omega'_{D_\kappa}(p)iT_c\right)$$

The autocorrelation function $r(i)$ depends on the relative time shift $i = i_{c1} - i_{c2}$. Since the PDF $\rho_{\chi(i_c)}$ of $\chi(i_c)$ is known, the autocorrelation function function can be evaluated analytically as,

$$r(i) = r(i_{c1} - i_{c2}) = E\left\{\exp\left(-jk'_{\phi_\kappa}(q)(\chi(i_{c1}) - \chi(i_{c2}))\right)\right\}$$
$$\qquad (7)$$
$$= \delta(i) + (1 - \delta(i))\left\|\Gamma(k'_{\phi_\kappa}(q))\right\|^2.$$

The function $\Gamma(k'_{\phi_\kappa}(q))$ can be identified as a radiation characteristic for the time modulated array. Furthermore, $\Gamma(k'_{\phi_\kappa}(q))$

is a function of the PDF $\rho_{\chi(i_c)}$. This can also be seen as the characteristic function of the PCM evaluated at $k'_{\phi_\kappa}(q)$,

$$\Gamma(k'_{\phi_\kappa}(q)) = E\left\{\exp\left(-jk'_{\phi_\kappa}(q)\chi(i_{c1})\right)\right\} \quad (8)$$
$$= \int_{-\infty}^{\infty} \rho_{\chi(i_{c1})} \exp\left(-jk'_{\phi_\kappa}(q)\chi(i_{c1})\right) d\chi(i_{c1}).$$

The result matches to array factor investigations [8]-[12], where the array factor is the Fourier Transform over the antenna weightings. Therefore, the PDF becomes a design parameter of the ambiguity function shape in angular direction and can be exploited for sidelobe suppression.

The periodogram $f_\chi(q,p)$ can be further evaluated,

$$f_\chi(q,p) = \left\|W(\omega'_{D_\kappa}(p))\right\|^2 \left\|\Gamma(k'_{\phi_\kappa}(q))\right\|^2 \quad (9)$$
$$+ W(0)(1 - \left\|\Gamma(k'_{\phi_\kappa}(q))\right\|^2)$$
$$= \mathcal{I}_c^2 \left(\left\|\frac{W(\omega'_{D_\kappa}(p))}{\mathcal{I}_c}\right\|^2 \left\|\Gamma(k'_{\phi_\kappa}(q))\right\|^2 \right.$$
$$\left. + \frac{1}{\mathcal{I}_c}\left(1 - \left\|\Gamma(k'_{\phi_\kappa}(q))\right\|^2\right)\right)$$

The function $W(\omega'_{D_\kappa}(p))$ is the DFT of the rectangular time window and $W(0) = \mathcal{I}_c$ denotes the signal energy. In order to construe the result of (9), the function $W(\omega'_{D_\kappa}(p))$ is normalized. Since the first term $\left\|\frac{W(\omega'_{D_\kappa}(p))}{\mathcal{I}_c}\right\|^2 \left\|\Gamma(k'_{\phi_\kappa}(q))\right\|^2$ has its maximum at the target position with an amplitude value of one, the latter term $\frac{1}{\mathcal{I}_c}(1 - \left\|\Gamma(k'_{\phi_\kappa}(q))\right\|^2)$ has a lower amplitude. In contrast to [7], the angle-Doppler coupling becomes a constant side lobe floor, denoted by the latter term in (9), rather than a Bessel function. Further, the latter term is a parasitic effect of the chosen random PCM approach. If the latter term vanishes, the angle-Doppler coupling is not longer present and therefore for a large number of chirps, the angle-Doppler coupling is minimal as it is demonstrated through simulations in Section IV.

IV. SIMULATION RESULTS

The simulation is carried out with $N = 4$ transmit antennas and $M = 4$ receive antennas, mounted in a collocated manner as depicted in Figure 2, such that the virtual MIMO array length is maximal. The FMCW chirp duration is set to $T_c = 10$ μs, while the carrier frequency is $f_0 = 77$ GHz and the angular bandwidth $B = 20\pi$ MHz. If two targets are present, the targets are at the same range bin in a distance of $r = 10$ m. The same distance $r = 10$ m is set for the single target simulation.

Figure 3 illustrates the sinus cardinal like characteristic of the main lobe and its sidelobes. This sinus cardinal characteristic arises from the uniform PDF, therefore the resolution is maximal, while the sidelobes are high. As a consequence, if the PDF is replaced by a Gaussian distribution, the resolution decreases and the sidelobes are suppressed, as it is illustrated in Figure 4. The uniform and Gaussian PDF are depicted in Figure 8 and Figure 9, respectively. Both PDF's are discrete, which illustrates the switching of the transmit array.
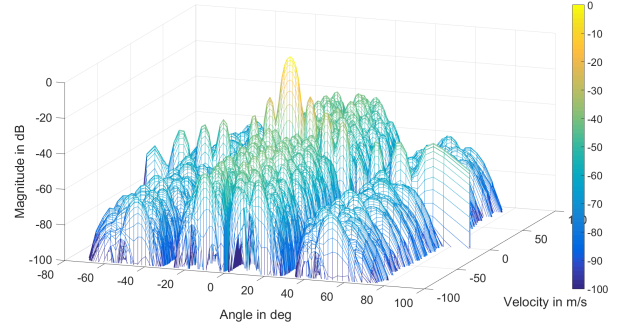
Fig. 3. Angle-Doppler AF for single target with $SNR = 10$ dB, $\mathcal{I}_c = 512$ and uniform PDF
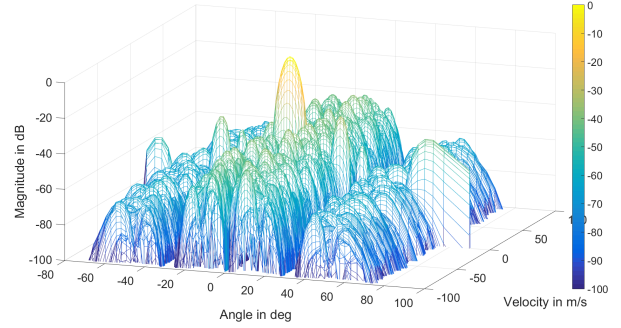
Fig. 4. Angle-Doppler AF for single target with $SNR = 10$ dB, $\mathcal{I}_c = 512$ and Gaussian PDF.
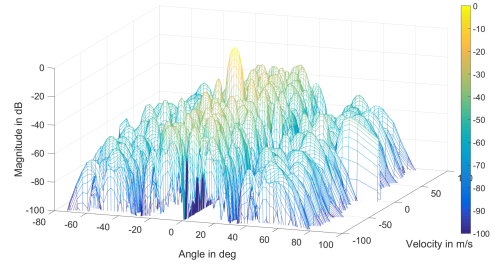
Fig. 5. Angle-Doppler AF for single target with $SNR = 10$ dB, $\mathcal{I}_c = 128$ and rectangular PDF.

Another degree of freedom by the proposed method is the choice of number of chirps, as it increases the sidelobe floor of the AF. The AF in Figure 5 has a higher sidelobe floor in comparison to the AF in Figure 3. As a result, as the number of chirps is increased, the influence of sidelobe floor on target detection decreases, because the sidelobes perturb the target detection much more than the sidelobe floor. Therefore, for a high number of chirps, the AF in Figure 3 performs similar in terms of sidelobes and resolution compared to the filled array case. This is clearly shown in Figure 6, where the performance of the proposed scheme is similar to that of filled array with 16 elements (having the same resolution as the considered virtual MIMO array, but with only 8 elements in total). For the filled array, beamforming is undertaken at the receiver.
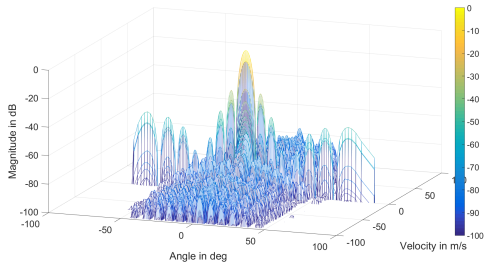
Fig. 6. Angle-Doppler AF for single target with $SNR = 10$ dB and $\mathcal{I}_c = 512$ using one transmitter and 16 receiver by applying conventional beamforming.
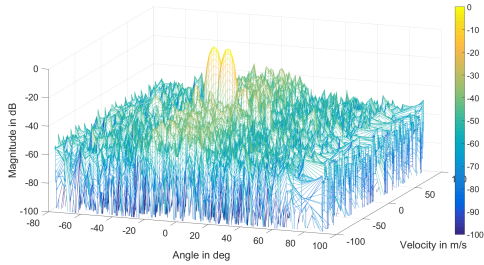
Fig. 7. Angle-Doppler AF for two target with $SNR = -20$ dB, $\mathcal{I}_c = 512$ and uniform PDF.
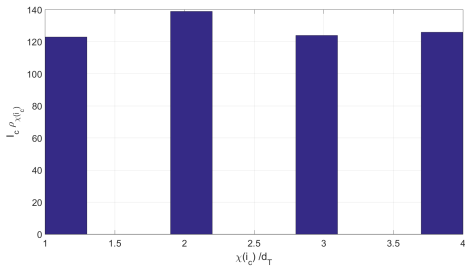
Fig. 8. Uniform discrete PDF for $\mathcal{I}_c = 512$ chirps.
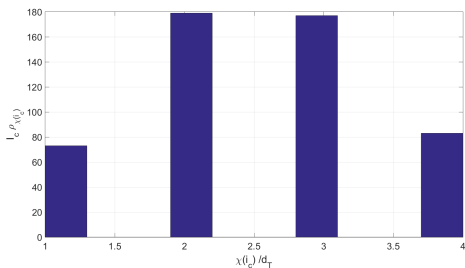
Fig. 9. Gaussian discrete PDF for $\mathcal{I}_c = 512$ chirps.

Figure 7 illustrates the method for a low Signal to Noise Ratio (SNR) in a multiple target scenario. The proposed matched filter approach enhances the detection performance for close proximity targets.

V. CONCLUSION

This work proposes a novel technique for enhanced low cost target detection with the objective of suppressing the angle-Doppler coupling. It considers PCM based on random spatio-temporal modulations of the transmit array followed by a matched filter processing at receiver. The ease of implementation, by just using a switched transmit array and a conventional beamforming technique at the receiver, makes the proposed approach attractive. Simulation results have proven the capability of the proposed method by illustrating the desired shaping of the AF based on the choice of the PDF of PCM. This provides for an additional degree of freedom in designing radar systems for target discrimination.

ACKNOWLEDGMENT

REFERENCES

[1] D. Bliss, K. Forsythe, G. Fawcett, "MIMO Radar: Resolution, Performance, and Waveforms," in *Proceedings of ASAP,* 2006.

[2] B. T. Perry, T. Levy, P. Bell, S. Davis, K. Kolodziej, N. O'Donoughue, J. S. Herd, "Low Cost Phased Array Radar for Applications in Engineering Education," in *IEEE International Symposium on Phased Array Systems and Technology,* 2013.

[3] Y. Tang, Y Lu, "Single transceiver-based time division multiplexing multiple-input-multiple-output digital beamforming radar system: concepts and experiments" in *IET Radar, Sonar and Navigation,* 2013.

[4] D. Zoeke, A. Ziroff, "Phase Migration Effects in Moving Target Localization Using Switched MIMO Arrays," in *Proceedings of the 12th European Radar Conference,* September 2015.

[5] A. Zwanetski, H. Rohling, "Continuous Wave MIMO Radar Based on Time Division Multiplexing," in *19th International Radar Symposium,* 2012.

[6] J. Guetlein, A. Kirschner, J. Detlefsen, "Motion Compensation for a TDM FMCW MIMO Radar System," in *Proceedings of the 10th European Radar Conference,* 2013.

[7] C. Hammes, Y. Nijsure, B. Shankar, U. Schröder, B. Ottersten, "Discrimination of Angle-Doppler Signatures using Arbitrary Phase Center Motion for MIMO Radars," in *IEEE Radar Conference,* 2017. (available online: http://wwwen.uni.lu/snt/people/christian_hammes).

[8] S. Yang, Y.-B. Gan, P. Khiang Tan, "Linear Antenna Arrays With Bidirectional Phase Center Motion," *IEEE Trans. Antennas Propag.,* vol. 53, no. 5, April 2005.

[9] G. Li, S. Yang, Z. Nie, "Direction of Arrival Estimation in Time Modulated Linear Array With Unidirectional Phase Center Motion," *IEEE Trans. Antennas Propag.,* vol. 58, no. 4, 2010.

[10] S. Yang, Y.-B. Gan, A. Qing, "Sideband Suppression in Time-Modulated Linear Arrays by the Differential Evolution Algorithm," *IEEE Antennas Wireless Propag. Lett.,* vol. 1, 2002.

[11] L. Poli, P. Rocca, L. Manica, A. Massa, "Pattern synthesis in time-modulated linear array through pulse shifting," *IET Microwave, Antennas and Propagation*, February 2009.

[12] J. Guo, S. Yang, S.-W. Qu, Jun Hu, Zaiping Nie, "A Study on Linear Frequency Modulation Signal Transmission by 4-D Antenna Arrays," *IEEE Trans. Antennas Propag.,* vol. 63, no. 12, December 2015.

[13] P. Setlur and M. Rangaswamy, "Waveform Design for Radar STAP in Signal Dependent Interference," *IEEE Trans. Signal Process.,* vol. 64, no. 1, January 2016.